

Proceedings of the 6th International Conference on

Optical Measurement Techniques for Structures & Systems III



The conference was organized within the framework of the Scientific Research Community OPTIMESS, supported by the Research Foundation-Flanders (FWO)

Antwerp, Belgium

8-9 April 2015



Joris Dirckx
Editor

© Copyright Shaker Publishing 2016

All rights reserved. No part of this publication may be reproduced, stored in a retrieval system, or transmitted, in any form or by any means, electronic, mechanical, photocopying, recording or otherwise, without the prior permission of the publisher.

Printed in Germany.

ISBN 978-90-423-0439-0

Shaker Publishing
St. Maartenslaan 26
NL 6221 AX Maastricht, The Netherlands
Tel.: 0031-43-3500424
Fax: 0031-43-3255090
[http:// www.shaker.nl](http://www.shaker.nl)

TABLE of CONTENTS

CONTRIBUTIONS / CHAPTERS

1. Sensing of in-plane displacement using circular grating Talbot interferometer – *Schilpi Agarwal* – p.1
2. Spectral radiance measurement at specific points of a light emitting diode – *Fiona Belfio* – p. 13
3. Production Monitoring of a RTM Automotive Control Arm by means of Fibre Optic Sensors – *Gabriele Chiesura* – p. 21
4. Recording and Processing Techniques for 3D Images of a Precision Optical Surface – *M.V. Chirkin* – p. 31
5. Projection-based polygon estimation in X-ray computed tomography – *Andrei Dabravolski* – p. 41
6. Fast flame temperature estimation using a point diffraction interferometer and non-negative least square method – *E. de la Rosa Miranda* – p. 51
7. Damage monitoring using Continuous Scanning LDV methods: numerical approach – *Dario Di Maio* – p. 61
8. Developments in Opto-Electronic Holography (OEH) for measurement of sound-induced eardrum motion – *Ivo Dobrev* – p. 73
9. Spectral ray tracing to model the spectrum of a luminaire equipped with an interference filter – *Guy Durinck* – p. 85
10. Transformer core vibration measurements by means of laser scanning vibrometer – *S. Gorji Ghalamestani* – p. 95
11. Digital Image Correlation measurements of jaw bending in living stag beetles – *Jana Goyens* – p. 107
12. Correction of laser Doppler vibrometry measurements affected by steering mirror vibration – *Ben Halkon* – p. 117

13. Wavefront-based active alignment of multi-element optical systems – *Reik Krappig* – p. 127
14. Characterization of butane flames under magnetic field using digital speckle pattern interferometry – *Manoj Kumar* – p. 137
15. Digital holography for measurement of natural convective heat transfer coefficient along the surface of electrically heated wire – *Varun Kumar* – p. 149
16. Modal analysis of a composite automotive component using fibre Bragg grating sensors embedded via Resin Transfer Moulding – *Alfredi Lamberti* – p. 161
17. Phase retrieval algorithm by fitting ellipses and computing Euclidean Distances – *Francisco Alejandro Lara-Cortes* – p. 171
18. Precise measurement of grinded aspherical and freeform optical surface shape by digital holography – *Vit Lédl* – p. 181
19. 3D deformation measurement with more than 2 cameras and digital image correlation: Approach, applications and benefit – *Ralf Lichtenberger* – p. 193
20. Identification of vibration modes from sub-microstrain Fiber-optic Bragg Grating data using an improved wavelength detection algorithm – *Patrizia Moretti* – p. 203
21. Microscopic laser triangulation in harsh industrial conditions for the inspection of microstructured surfaces – *Thomas Mueller* – p. 215
22. Fringe projection profilometry applications: preliminary results for measurements of a swordfish – *A. Nava Vega* – p. 225
23. Defining geometrical position information of a thermal camera and object curvatures using thermography – *Jeroen Peeters* – p. 233
24. Holographical arrangement employing frequency and phase modulation of reference wave in time average digital holographic interferometry – *Pavel Psota* – p. 243

25. Profiling oil-water flows in microchannel: preliminary results using Optical Feedback Interferometry – *E. E. Ramirez-Miquet* – p. 251
26. Low cost automated setup for fringe projection profilometry – *Uriel Rivera-Ortega* – p. 259
27. Applications and interpretations in laser vibrometry: confident steps in the light direction – *Steve Rothberg* – p. 267
28. Fiber-coupled interferometric sensor for high-speed measurement of optical surfaces – *Markus Schulz* – p. 277
29. Real-time 3D lensless imaging through scattering media – *Alok Kumar Singh* – p. 289
30. Comparative study of NDT inspection methods - Part A: defect tracing in Carbon Fiber Composite Laminates – *Gunther Steenackers* – p. 297
31. Sand movement in a sand-bed scour hole – *Takayuki Tsutsui* – p. 305
32. Accurately measuring 2D position using a composed grid pattern and DTFT – *Sam Van Dam* – p. 313
33. Real-time phase unwrapping in Fourier space using a graphics processing unit – *Sam Van der Jeught* – p. 321
34. A dynamic region estimation method for cerebral perfusion CT – *Geert Van Eyndhoven* – p. 331
35. Dynamic Flat field correction in X-ray computed tomography – *Vincent Van Nieuwenhove* – p. 343
36. Using super-resolution images to improve the measurement accuracy of DIC – *Yueqi Wang* – p. 353
37. Visual flow measurement using a fiberscope system combined with twinkling laser light sheet technique – *Yoshifumi Yokoi* – p. 363

Fast flame temperature estimation using a point diffraction interferometer and non-negative least square method

E. de la Rosa Miranda^a, L. R. Berriel-Valdos^b E. Gonzalez-Ramirez^a, Carlos Olvera Olvera^a, Tonatiuh Saucedo Anaya^c, J. G. Arceo Olague^a and Ismael de la Rosa Vargas^a

Abstract

Some of the interferometry methods proposed for flame temperature measurements from its projection could be complex and demand so much computing time. Assuming a circular symmetric and smooth flame temperature distribution, it is possible to use a linear combination of Gaussian functions with weights constrained to non-negative values.

Contact information

^a edelarosam@hotmail.com

Unidad Académica de Ingeniería Eléctrica, Universidad Autónoma de Zacatecas,
Antiguo Camino a la Bufa No. 1, Col. Centro. C. P. 98000, Zacatecas, Zac. México

^b berval@inaoep.mx

Instituto Nacional de Astrofísica y Óptica y Electrónica
Luis Enrique Erro No. 1, Santa María Tonantzintla, San Andrés Cholula, C.P. 72840, Puebla,
México

^c tsaucedo@fisica.uaz.edu.mx

Unidad Académica de Física, Universidad Autónoma de Zacatecas,
Paseo a la Bufa S/N, Col. Centro. C. P. 98000, Zacatecas, Zac. México

Introduction

The temperature of an object is a measure of the thermal energy. It represents the total internal energy of the object. In general, temperature is determined by measuring an optical, mechanical or electrical property of a material that varies with temperature. Temperature measurements using mechanical and electrical techniques are effective when the object is solid with homogeneous temperature and the sensor is in thermal equilibrium. For non-solid objects like flames, these techniques present several problems, Yilmaz et al [1], e.g., a great number of measurements are required to obtain the total volumetric temperature of the flame and the its temperature distribution is modified by the sensors. On the other hands , optical methods do not perturb the flame temperature and also they allow to have a bigger set of measurements.

Several optical methods are based on color [2, 3], infrared [4], and interferometric [2, 5, 6] techniques. Interferometric methods are widely used to measure deformation, tension, temperature, etc [7, 8] in a non-invasive and non-destructive way. Such magnitudes produce a frequency modulated fringe pattern called interferogram. Demodulation and phase inversion processes are needed to estimate the desired physical magnitude. Most of the phase recovering methods are based on the Fourier Transform [9], phase shifting [10] or regularization [11-13] techniques. Techniques for phase recovery such as Fourier based produces a wrapped phase in the interval $(-\pi, \pi)$. To unwrap this phase, path dependent algorithms [14] can be applied. Ghiglia et. al. shows a simple test for path dependence [15]. A robust alternative for many cases is the least-squares solution, which is described in matrix form by Hunt [16]. Another robust algorithm to find a solution in the presence of path-integral phase inconsistencies using the cosine transform is that proposed by Ghiglia and Romero [17]. Optical tomography is a method used to obtain the spatial distribution of the refraction index of a phase object (PO) on its non refractive index (refractionless limit) from one or more projections. For the case of radially symmetrical phase objects only one projection is necessary to reconstruct the refractive index distribution. This projection is formed by a set of summa rays (Figure 1). Tomographic reconstruction methods can be grouped into two categories: back projection methods and algebraic methods (ART) [18, 19, 20, 21]. In the algebraic method, the projections are a linear transformation of the cross sections of the object, i.e., a linear system given by the vector solutions (projection of each section), a transformation matrix and a vector of unknowns (cross section of the linear system phase object) [7, 18, 19, 20, 21]. The number of unknowns can be reduced assuming the temperature distribution in each section can be estimated by a linear combination of basis functions. In this paper, we present a simple and rapid method for measuring the temperature of a flame, using a point diffraction interferometer and a set of basis functions.

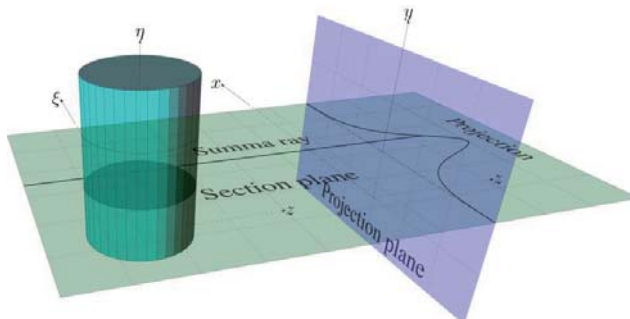


Figure 1: Object projection.

Base theory

Interferometry

Interferometry techniques are used to measure physical quantities [1, 7] such as temperature, pressure, tension or deformation associated to the refraction index of a object. A common objective of these methods is to produce a fringe pattern modulated by variations of these magnitudes. An interferogram is described mathematically by

$$I(x, y) = a(x, y) + b(x, y) \cos[2\pi f_0 x + \phi(x, y)] \eta_m(x, y) + \eta_a(x, y), \quad (1.1)$$

where (x, y) are spatial coordinates, $a(x, y)$ is the background illumination, $b(x, y)$ is the amplitude modulation, $\phi(x, y)$ is the phase associated to the refraction index, f_0 is the carrier frequency [9], and $\eta_m(x, y)$ and $\eta_a(x, y)$ are the multiplicative and additive noises, respectively; in the case of Speckle Pattern Interferometry (SPI) [21] or single path interferometry [7], the noise is multiplicative. For higher levels of noise it is necessary the use of a filter to preserve fringes. In many cases $a(\cdot)$ and $b(\cdot)$ are considered as constants when they vary slowly. For interferogram with no carrier ($f_0 = 0$) the interferogram can be rewritten as

$$I(x, y) = \cos[\phi(x, y)] \eta_m(x, y) + \eta_a(x, y), \quad (1.2)$$

The optical path length (OPL) of one ray through a transparent medium is described by

$$OPL = \int_C n ds \quad (1.3)$$

OPL is along path C. When refraction is not significant, the path can be approximated by a straight line. If the beam is propagated along the z axis, as it is shown in Figure 2, the OPL can be expressed as:

$$OPL = \int_C n(z) dz \quad (1.4)$$

The optical path difference (OPD) $\Delta(\cdot)$ is given by

$$\Delta(\cdot) = \int_C [n(\cdot) - n_0] dz, \quad (1.5)$$

where n_0 is the refraction index of the medium. The OPD is related to the phase ϕ in Equation 1.2 by:

$$\Delta(x) = \frac{2\pi}{\lambda} \phi(x) \quad (1.6)$$

For circularly symmetric optical paths (OP), Equation 1.6 can be expressed in terms of Abel Transform [7], $A\{f\}$ by

$$A\{n(r)\} = A\{n_0\} = A\{n_d(r)\} = 2 \int_0^{+\infty} \frac{n_d(r)}{\sqrt{r^2 - z^2}} dr \tag{1.7}$$

where r is given by $\sqrt{z^2 + x^2}$.

One of the simplest approaches to find Abel transform of a circularly symmetric discrete function ($n_k = n(k), k \in \mathbb{Z}$), is by a linear combination of rings of width Δr and height f_k . The discrete Abel Transform, $A\{n_k\}$, can be obtained by

$$N_k = A_d\{n_k\} = 2 \sum_{k=1}^{r_k+1} n_k \frac{r}{(r^2 - k^2)^{\frac{1}{2}}} dr \tag{1.8}$$

Solving the integral we obtain:

$$\frac{N_k}{2r} = \sum_{k=i} A_{i,k} n_k \tag{1.9}$$

where $A_{i,k} = \left[(k+1)^2 - i^2 \right]^{\frac{1}{2}} - \left[k^2 + i^2 \right]^{\frac{1}{2}}$.

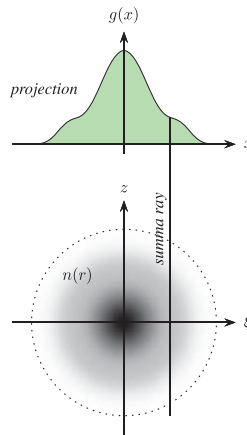


Figure 2: Cross section object projections. OPL is calculated along the straight line.

Function approximation using base functions

The purpose of interpolation is to obtain a function which best fits a set of points using a predefined cost function. The approximation process can be set as follows: Given a set of points

$\{(x_i, y_i) | x_i, y_i \in \mathbb{R}, i \in \mathbb{Z}^+\}$ find a function, $f(x)$ such that

$$\min_i \|y_i - f(x_i)\|^2 \tag{1.10}$$

which $f(x)$ could be a linear combination of basis functions

$$f(x) = \sum_j w_j g_j(x_i), \tag{1.11}$$

where the set of weights $\{w_j | w_j \in \mathbb{R}\}$ are those which optimize Equation 1.12.

$$\min_{\{w_j\}} \left\| \sum_i y_i w_j g_j(x_i) \right\|_{\mathbb{R}, j}^2 \quad (1.12)$$

Point Diffraction Interferometer

In Figure 3, the interferometer of common path uses a diffractor element to measure the wavefront [22]. The Point diffraction interferometer (PDI) is located at the focus L_2 . The PDI is a thin optical disc half the diameter of an Airy Disk, equal to $1.22 \lambda f\#$, where λ is wavelength, $f\#$ is the incident wavefront numeric aperture. The disk modulates the transmitted beam amplitude and phase. The PDI generates a synthetic wavefront superimposed to the original wavefront [5, 22, 23]. The basic idea of the PDI is shown in Figure 4, where the reference wavefront and the object produce an interferogram.



Figure 3: Interferometer setup.

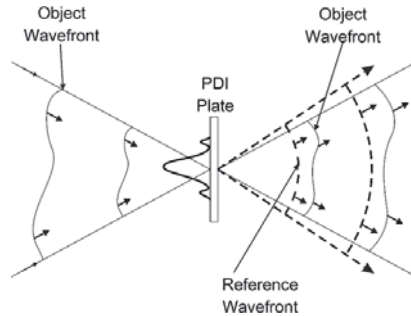


Figure 4: PDI Incident (object) and transmitted wavefront (Reference and Object).

Proposed reconstruction method

If PO is a smooth phase object, then, its refraction index $(n(r))$ can be approximated by a linear combination of k basis functions defined by Equation 1.11 and Equation 1.7 can be rewritten as

$$\begin{aligned} \phi(r) &= A \left\{ \sum_k w_k f_k(r) \right\} = 2 \int \frac{\sum_k w_k f_k(r)}{\sqrt{r^2 - \lambda^2}} \\ \phi(r) &= \sum_k w_k A \{ f_k(r) \} = \sum_k w_k F_k(x) \end{aligned} \quad (1.13)$$

or in matrix form:

$$\mathbf{g} = \mathbf{F}\mathbf{w} \tag{1.14}$$

One choice for the set of basis functions is a set of Gaussians. The positions of the gaussians can be evenly distributed on an interval L . The width σ of the Gaussian functions f may be determined by the following relationship

$$\sigma = \frac{L}{2d + (n_g - 1)s} \tag{1.15}$$

where d is the distance of the lower limit to the center of the first Gaussian, s is the separation between gaussians (depending on σ) and n_g is the number of Gaussians (see Figure 5).

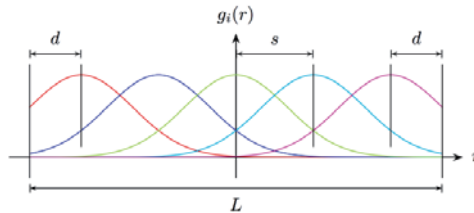


Figure 5: Uniformly distributed (over an interval L) basis functions

The optimal weights w^* that fulfill Equation 1.14, produce oscillations that make $n_d(r) < 0$. Therefore, it is necessary to limit the solution to weights, w_k , equal or greater than zero, i.e.

$$\min_w \left\| \mathbf{F}\mathbf{w} \right\|^2, \quad \mathbf{w}_k \geq 0 \tag{1.16}$$

To find the solution of Equation 1.16 the non-negative least square method can be used.

Results

To show the reconstruction quality, a test function is used. This function is expressed as

$$\eta_t(r) = 10^{-4} \left[\exp(-5r^2) + \exp\left(-\frac{5}{9}r^2\right) \right] \tag{1.17}$$

Figure 6 shows some constrained and non-constrained approximations. To compare results, in both approximations we use different number of basis functions (BF). We found that the constrained approximation has a very good fitting to the test function when it uses a linear combination of 5 basis functions; with a higher number of BF, error change is not significant. Also we can see that the non-constrained approximations goes below the value of “0”, such thing does not happen in the case of the constrained approximation.

Figure 7 shows an interferogram obtained with a PDI and a 532.8 nm-wavelength laser. A simple rotation is applied to the interferogram to see vertically. The temperature (T) is found by using the Gladstone-Dale relationship [7]

$$n - 1 = \frac{0.294036 \times 10^{-3}}{1 + 0.369203 \times 10^{-2} T} \tag{1.18}$$

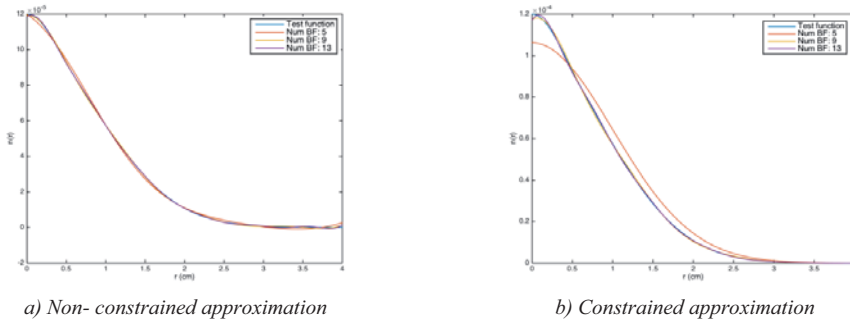


Figure 6: Functions approximation, $n_g = \{5, 9, 13\}$, $d = 0$ y $s = 1$.

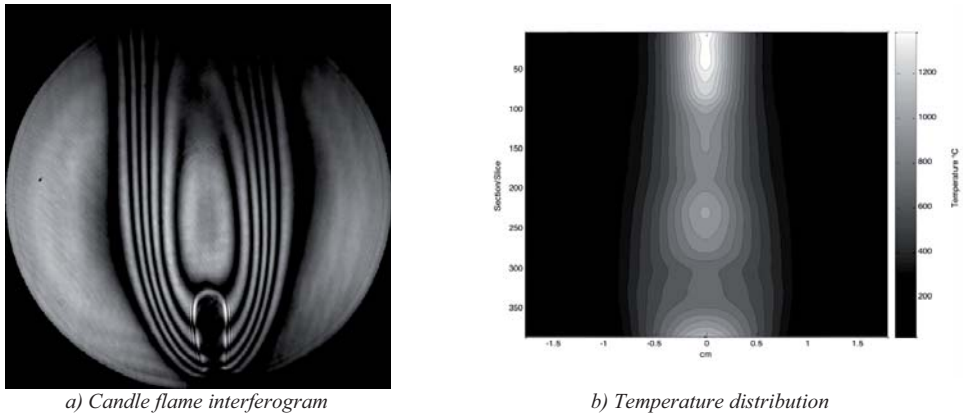


Figure 7: Interferogram and temperature distribution of a candle flame.

Conclusion

We have shown a temperature estimation method for the optical tomographic reconstruction using only one projection of a smooth phase object. With this method we can obtain any longitudinal or cross-sectional section of the volumetric distribution of the temperature of a candle flame.

Acknowledgements

We want to thank the Universidad Autónoma de Zacatecas (P/PROFOCIE-2014-32MSU0017H-09), the National Institute of Astrophysics, Optics and Electronics, for all the support for this work.

References

- [1] Nadir Yilmaz, Walt Gill, A. Burl Donaldson, and Ralph E. Lucero. Problems encountered in fluctuating flame temperature measurements by thermocouple, *Sensors*, 8(12): 7882–7893, (2008).
- [2] Xudong Xiao, Ishwar K. Puri, and Ajay K. Agrawal. Temperature measurements in steady axisymmetric partially premixed flames by use of rainbow schlieren deflectometry. *Appl. Opt.*, 41(10), 1922–1928, (Apr 2002).
- [3] P.M. Brisley, Gang Lu, Yong Yan, and S. Cornwell. Three-dimensional temperature measurement of combustion flames using a single monochromatic ccd camera. *Instrumentation and Measurement, IEEE Transactions on*, 54(4), 1417–1421, (Aug 2005).
- [4] Hiroki Uchiyama, Masato Nakajima, and Shinichi Yuta. Measurement of flame temperature distribution by ir emission computed tomography. *Appl. Opt.*, 24(23):4111–4116, (Dec 1985).
- [5] Juan C. Aguilar, Luis Raul Berriel-Valdos, and Jose Felix Aguilar. Measuring of temperatures of a candle flame using four multidirectional point diffraction interferometers. *Optical Engineering*, 52(10): 104103–104103, (2013).
- [6] C. Alvarez-Herrera, D. Moreno-Hernández, and B. Barrientos-García. Temperature measurement of an asymmetric flame by using a schlieren system. *Journal of Optics A: Pure and Applied Optics*, 10(10):104014, (oct 2008).
- [7] Charles M. Vest. *Holographic Interferometry*, (John Wiley & Sons, NewYork, 1979).
- [8] K. J. Gasvik. *Optical Metrology*, (Wiley, New York, 1987).
- [9] Mitsuo Takeda, Hideki Ina, and Seiji Kobayashi. Fourier-Transform Method of Fringe-Pattern Analysis for Computer-Based Topography and Interferometry. *Journal of Optical Society of America A*, 72:156–159, (1981).
- [10] D. Malacara, M. Servín, and Z. Malacara. *Interferogram Analysis for Optical Testing*, (Marcel-Dekker, Inc., New York, 1998).
- [11] Jesús Villa, Ismael de la Rosa Gerardo Miramontes, and Juan Antonio Quiroga. Phase recovery from a single fringe pattern using an orientational vector field regularized estimator. *Journal of Optical Society of America A*, 22, 2766–2773, (2005).

- [12] L. Guerriero, G. Nico, G. Pasquariello, and S. Stramaglia. New regularization scheme for phase unwrapping. *Applied Optics*, 37(14), 3053–3058, (1998).
- [13] M. Rivera and J. L. Marroquin. Half-quadratic cost functions for phase unwrapping. *Optics Letters*, 29(5), 504–506, (2004).
- [14] B. Ströbel. Processing of interferometric phase maps as complex-valued phasor images. *Applied Optics*, 35, :2192–2198, (1996).
- [15] D.C. Ghiglia and M.D. Pritt. *Two-dimensional phase unwrapping: theory, algorithms, and software*, (Wiley-Interscience, 1998).
- [16] B. R. Hunt. Matrix formulation of the reconstruction of phase values from phase differences. *J. Opt. Soc. Am.*, 69(3), 393–399, (Mar 1979).
- [17] Dennis C. Ghiglia and Louis A. Romero. Robust Two-Dimensional Weighted and Unweighted, Phase Unwrapping for Uses Fast Transform and Iterative Methods. *Journal of Optical Society of America A*, 11, 107–117, (1994).
- [18] S. R. Deans. *The Radon Transform and Some of its Applications, first edition*, (Wiley, 1983).
- [19] R.M. Lewitt. Reconstruction algorithms: Transform methods. *Proceedings of the IEEE*, 71(3), :390–408, March 1983.
- [20] H.J. Scudder. Introduction to computer aided tomography. *Proceedings of the IEEE*, 66(6), 628–637, (June 1978).
- [21] A. K. Jain. *Fundamental of Digital Image Processing. Information and System Science*, (Prentice Hall, 1989).
- [22] D. Malacara. *Optical Shop Testing* (Wiley Series in Pure and Applied Optics, 2007).
- [23] Millerd, James E. and Brock, Neal J. and Hayes, John B. and Wyant, James C., Instantaneous phase-shift point-diffraction interferometer, *Proc. SPIE*, 5531, 264-272 (2004).